Convection in Weld Pool and Its Effect on Penetration Shape in Stationary Arc Welds†

Akira MATSUNAWA*, Shinichiro YOKOYA**, Yutaka ASAKO***

Abstract

The importance of convective heat transfer in the weld pool has been widely recognized in relation to the penetration shapes of base metal. The main causes that associate streaming in molten pool are the electro magnetic force, buoyancy force, surface tension and aero dynamic drag force. But, the mechanism of heat transfer has not yet been clarified well. Therefore, in this work, they have paid special attension on the importance of convectional heat transfer in the weld pool and the anode size or heat source size under the same heat input, or same current value. A finite difference methode was employed to solve above-mentioned mechanism. The results obtained were as follows.

1) When arc length is short, the velocity field induced by outward surface shear stress consists of two flow loops of opposite directions in the molten pool, which lead to comparatively deep weld shape.

2) In case of short arc length and positive temperature coefficient of surface tension, surface tension is predominant. Accordingly, penetration shape is deep.

3) In case of long are length, aero dynamic drag force is predominant, which leads to a 'shallow' center and 'deep' peripheral penetration.

KEY WORD: (Heat transfer) (Mass transfer) (Surface tension) (Plasma stream) (Convection) (Electromagnetic force) (Penetration shape) (Arc welding) (Free boundary problem)

1. Introduction

The importance of liquid motion in weld pool which gives considerable effects on the weld penetration shape has been recognised recently. Several works have been published concerning numerical calculation of weld pool streaming but comprehensive conclusion has not yet been established.

In this study, the authors have paid special attention to convectional modes in the weld pool, and conducted numerical analysis of heat and mass transfer in the stationary TIG arc weld pool. There are four motive forces which may induce convectional flow in the weld pool. They are (1) electro magnetic force (E) which generates axitial flow due to divergent current flow, that is, pinch effect, (2) buoyancy force (B) which brings convection through temperature distributions, or the density distribution in the weld pool, (3) surface tension (S) which induces convection due to temperature differences on the free surface, and (4) aero-dynamic drag force (A) which causes radial surface flow by arc plasma stream. Various penetration patterns seem to be produced by different heat transfer due to different convectional modes.

Some works have been done about heat and mass transfer by various convectional modes in fixed vessel. Typical published works are those by Matsunawa and his coworkers[1, 2, 3] and Oreper[4].

Recently, Oreper [5] conducted transient analysis considering surface tension, buoyancy force, and electromagnetic force under consideration of moving boundary. Results obtained were as follows; (1) the broadly distribted head flux and corresponding current distribution cause a situation where both electromagnetic and buoyancy forces are important in determing the fluid flow; however, in these systems the fluid flow fields does not play a significant role in defining the heat-transfer process. (2) heat flux and current density play an important role in determing the shape of the weld pool. (3) surface tension driven flow may produce quite high surface velocities and can have a profound effect on determing the weld pool

† Received on Nov. 4, 1987

* Professor, Welding Research Institute, Osaka University

** Collaborative Researcher, Associate Professor, Nippon Institute of Technology

*** Associate Professor, Tokyo Metroporitan University

Transactions of JWRI is published by Welding Research Institute of Osaka University, Ibaraki, Osaka 567, Japan

shape. Kou and Sun[6] also conducted numerical analysis considering buoyancy, electromagnetic force and surface tension as motive forces using moving boundary method, solving energy equation by enthalpy method. Nishiguchi and Ohji[7] have studied the convection in the weld pool or liquid pool in the hemispherical vessel, and deduced that arc plasma stream and electromagnetic force are main motive factors for the convection in a weld pool. There are other several works published about numerical calculation of weld pool streaming considering some of the above mentioned factors, but a comprehensive conclusion has not yet been established.

Furthermore, calculated result do not explain some of experimetal facts such as "deep periphery and shallow center" penetration which sometimes occur in TIG welding.

Therefore, in this work, the authors have paid special attention on the anode size or heat source size under the same heat input, or same current value. A finite difference method[8] was employed to solve three basic equations, i.e., the continuity equation, generarized Navier-Stokes equation which includes electro magnetic force, buoyancy force, surface tension and aero dynamic drag force, and energy equation considering arc heat input. And then they have obtained velocity field, temperature field, change of fusion boundary in case of pure heat conduction and convective heat transfer caused by single and combined effect of each force (including both negative and positive temperature coefficients of surface tension). In this paper, discussions are made on mechanism of heat and mass transfer with stationary TIG arc weld pool.

2. Simulation Model and Governing Equation

2.1 Plasma stream and shear stress on liquid surface

Shear stress of plasma stream on flat liquid surface of molten pool, and its dependence on arc length are calculated under the boundary conditions shown in **Fig. 1** and the following assumptions.

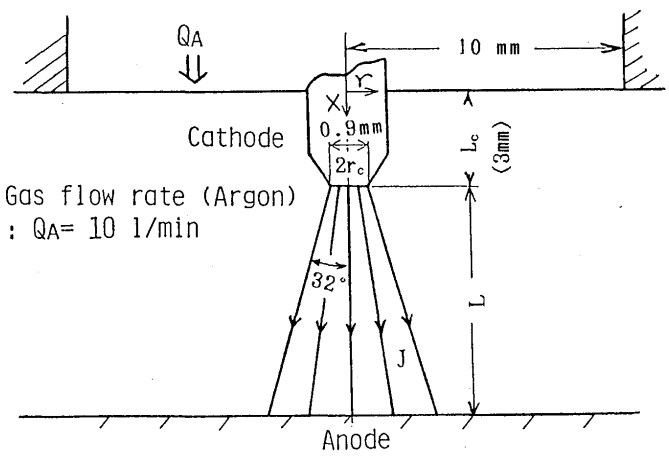

Fig. 1 Schematic diagram of stationary TIG arc model.

Table 1 Symbol and material constants

u	:	x-component velocity
v	:	r-component velocity
r	:	Radius from origin
ρ	:	Density (0.05kg/m^3)
μ	:	Coefficient of viscosity (2.9 x 10^{-4}kg/ms)
χ	:	Permiability (4π x 10^{-7}Wb/Am)
θ	:	Divergent angle of arc
I	:	Current (200A)
J	:	Current density (A/m^2)
α	:	Maximum divergent angle of arc (32°)
B_ϕ	:	Magnetic flux density (W$_b$/m^2)

(1) The arc is steady, rotationally symmetric and the flow is laminar.
(2) The values of physical properties used are at 10,000 K.

Equation of plasma motion is given as follows using symbols and units tabulated in **Table 1**.

Current density and magnetic field:

$$J = \frac{I}{2\pi((X - L_c + r_c/tan\theta)^2 + r^2)(1 - cos\alpha)} \tag{1}$$

$$B_\phi = \frac{XI(1 - cos\,\theta)}{2\pi((X - L_c + r_c/tan\,\theta)^2 + r^2)^{0.5}(1 - cos\alpha)sin\,\theta} \tag{2}$$

Continuity equation:

$$\frac{\partial \rho}{\partial t} + \frac{\partial}{\partial x}(\rho u) + \frac{1}{r}\frac{\partial}{\partial r}(r\rho v) = 0 \tag{3}$$

Motion equation:

x-component:

$$\frac{\partial}{\partial t}(\rho u) + \frac{\partial}{\partial x}(\rho uu) + \frac{1}{r}\frac{\partial}{\partial r}(r\rho vu) = -\frac{\partial p}{\partial x} + \frac{\partial}{\partial x}(\mu\frac{\partial u}{\partial x}) + \frac{1}{r}\frac{\partial}{\partial r}(r\mu\frac{\partial u}{\partial r}) + J_r \cdot B_\phi \tag{4}$$

r-component:

$$\frac{\partial}{\partial t}(\rho v) + \frac{\partial}{\partial x}(\rho uv) + \frac{1}{r}\frac{\partial}{\partial r}(r\rho vv) + \frac{\mu v}{r^2} = -\frac{\partial p}{\partial r} + \frac{\partial}{\partial x}(\mu\frac{\partial v}{\partial x}) + \frac{1}{r}\frac{\partial}{\partial r}(r\mu\frac{\partial v}{\partial r}) - J_x \cdot B_\phi \tag{5}$$

2.2 Governing equations of liquid motion containing various motive forces in the molten pool.

The following equations are given under the boundary condition as shown in **Fig. 2** using symbols and units tabulated in **Table 2**.

The equation of electromagnetic force (E) can be expressed in x–r coordinates as follows by transforming Sozou's method [9].

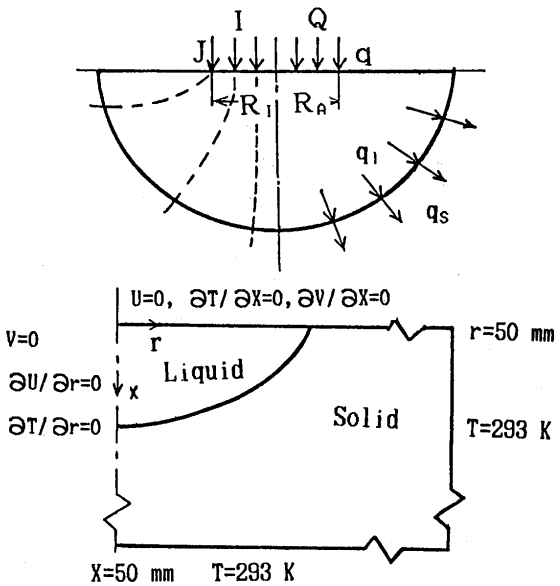

Fig. 2 Boundary condition for the calculation of temperature and velocity.

Table 2 Boundary condition and material constants

R_A	: Radius of heat source,	; R_A = 2 & 5 mm
R_I	: Anode radius,	; R_I = 1.1 mm, 2 mm & 5 mm
Q	: Total heat input,	; $Q = \pi R_A{}^2$ = 1570 J/s
q	: Heat flux intensity,	; $q = 2 \times 10^4$ & 1.25×10^5 kJ/m²s
j	: Current density,	; j = 52.6, 15.91 & 2.55 MA/m²
T_M	: Melting point,	; T_M = 1,809 K
ρ	: Density; 7.13×10^{-3} kg/cm³	
μ	: Coefficient of viscosity; 4×10^{-3} kg/(m·sec)	
χ	: Peamiability; $4\pi \times 10^{-7}$ W_b/Am	
β	: Coefficient of heat expansion; 1.4×10^{-4}	
$\partial\sigma/\partial T$	: Thermal coefficient of surface tension; –0.3 & 0.36 mN/(mK); by Mills [10]	
τ_P	: Shear stress on weld pool surface	
λ	: Heat condustivity; 0.041868 kJ/(m·s·K)	
T	: Temperature of liquid and solid phase	
H	: Enthalpy	

$$R^2 = r^2 + x^2$$

$$\zeta = \sqrt{\frac{R^2 - R_I{}^2}{2R_I{}^2} + \sqrt{\frac{X^2}{R_I{}^2} + \frac{(R_I{}^2 - R^2)^2}{4R_I{}^4}}} \tag{7}$$

$$\eta = x/(R_I\zeta) \tag{8}$$

x-component:

$$E_x = \frac{\chi I^2(1-\eta)\zeta}{4\pi^2 R_I{}^3(\zeta^2+\eta^2)(\zeta^2+1)} \tag{9}$$

r-component:

$$E_r = \frac{\chi I^2(\eta-1)\eta}{4\pi^2 R_I{}^3(\zeta^2+\eta^2)(\zeta^2+1)} \sqrt{\frac{1+\zeta^2}{1-\eta^2}} \tag{10}$$

Continuity equation:

$$\frac{\partial\rho}{\partial t} + \frac{\partial}{\partial x}(\rho u) + \frac{1}{r}\frac{\partial}{\partial r}(r\rho v) = 0 \tag{11}$$

Buoyancy force in molten pool:

$$F_B = \rho g \beta (T - T_M)$$

Surface tension is given as

$$F_s = \frac{\partial\sigma}{\partial T} \cdot \frac{\partial H}{\partial r} \cdot \frac{1}{dx \cdot C_p} \tag{12}$$

Aero dynamic drag force due to plasma stream:

$$F_p = \tau_p/dx$$

Motion equation:

x-component:

$$\frac{\partial}{\partial t}(\rho u) + \frac{\partial}{\partial x}(\rho u u) + \frac{1}{r}\frac{\partial}{\partial r}(r\rho v u)$$
$$= -\frac{\partial p}{\partial x} + \frac{\partial}{\partial x}\left(\mu\frac{\partial u}{\partial x}\right) + \frac{1}{r}\frac{\partial}{\partial r}\left(r\mu\frac{\partial u}{\partial r}\right) + E_x + F_B \tag{13}$$

r-component:

$$\frac{\partial}{\partial t}(\rho v) + \frac{\partial}{\partial x}(\rho u v) + \frac{1}{r}\frac{\partial}{\partial r}(r\rho v v) + \frac{\mu v}{r^2}$$
$$= -\frac{\partial p}{\partial r} + \frac{\partial}{\partial x}\left(\mu\frac{\partial v}{\partial x}\right) + \frac{1}{r}\frac{\partial}{\partial r}\left(r\mu\frac{\partial v}{\partial r}\right) + E_r + F_s + F_p \tag{14}$$

Heat input per unit volume is:

$$q_{in} = q/dx$$

Energy equation:

$$\frac{\partial}{\partial t}(\rho H)+\frac{\partial}{\partial x}(\rho u H)+\frac{1}{r}\frac{\partial}{\partial r}(r\rho v H)$$

$$=\frac{\partial}{\partial x}\left(\frac{\lambda}{C_p}\frac{\partial H}{\partial x}\right)+\frac{1}{r}\frac{\partial}{\partial r}\left(\frac{\lambda}{C_p}r\frac{\partial H}{\partial r}\right)+q_{in} \quad (15)$$

3. Boundary conditions and numerical method

Figure 3 shows the relation between (H) entalpy and (T) temperature of pure steel. To maintain continuity of calculation, the H–T relationship is assumed linear in the region where the solid and liquid phases coexist, i.e., the mushy zone. The liquid phase is defined when H is over 1,298 J/kg. The flow is assumed to be rotationally symmetric and laminar. The effective viscosity of solid phase was taken as 2.5 x 10^{13} times of the viscosity of liquid phase. A method adopted in this chapter is similar to Kou's method[6]. Figure 2 shows boundary condition to calculate the velocity and temperature fields as well as penetration shape.

In order to improve the accuracy of calculation, grids of variable spacing were used, i.e., finer spacing near the heat source and coaser away from it.

4. Results and discussion

Figure 4 shows influence of arc length on stream line in arc space and shear stress field on anode surface. If arc length is short, the convection is limited just beneath the cathode, on the other hand, in case of long arc length, there is a uniform streaming that flows out from inlet to outlet along the anode surface. Therefore, the longer the arc length is, the wider the shear stress acts on the pool surface.

Figures 5 and **6** show changes of penetration shapes with time after arc initiation and the distribution of isothermals and velocity after 60 seconds. Figure 5 shows the individual effect of each motive force, while Fig. 6 represents the combined effects on penetration shape and temperature/velocity fields.

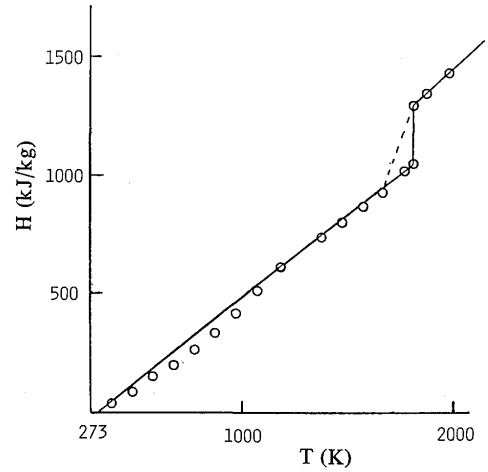

Fig. 3 Relationship of temperature and enthalpy [11]

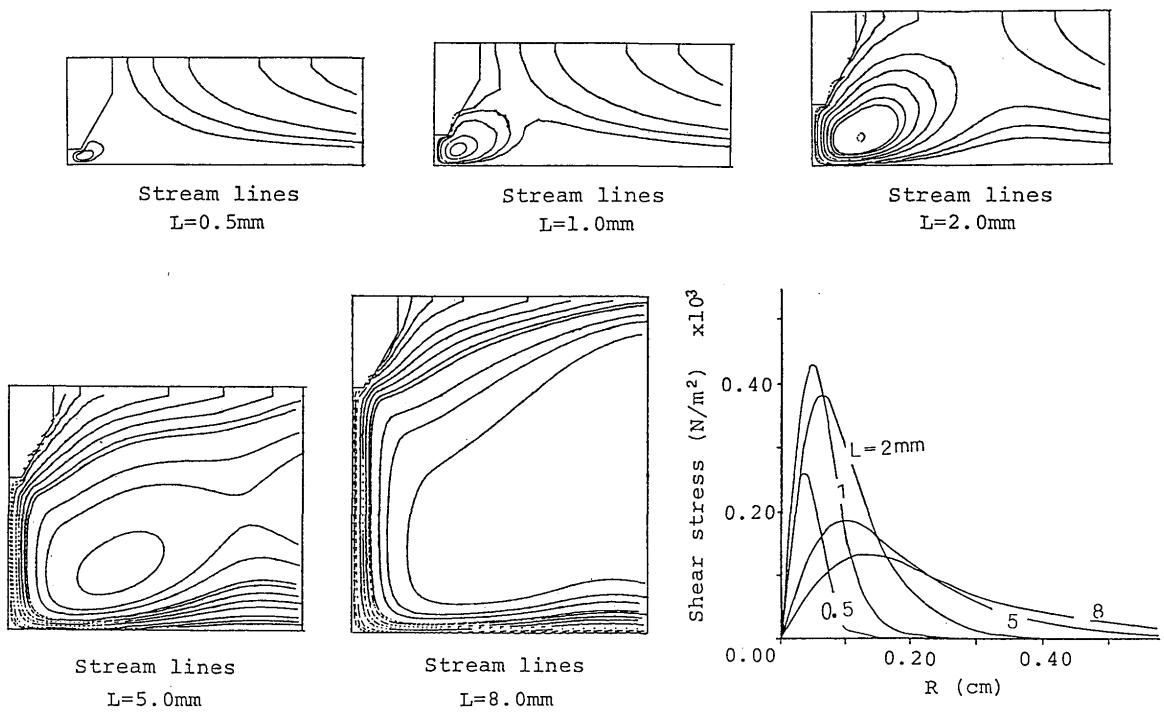

Fig. 4 Influence of arc length on stream line and shear stress field on anode surface.

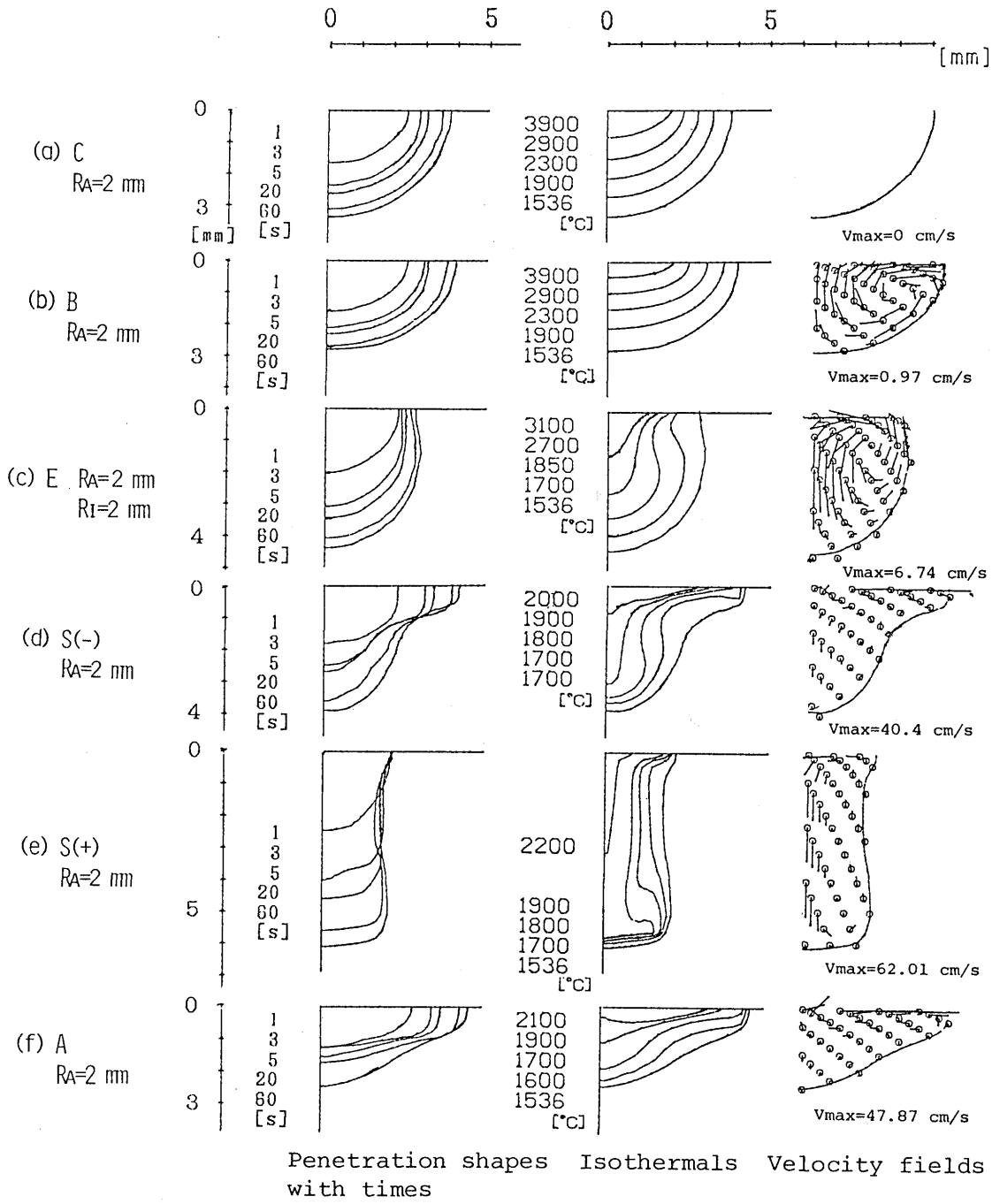

Fig. 5 Penetration shapes with times, temperature and velocity fields due to (a) pure conduction, (b) buoyancy force, (c) electromagnetic force and surface tension (including both (d) negative and (e) positive temperature coefficients of surface tension), and (f) aero dynamic drag force for the case : Q = 1570J/s, I = 200A, respectively.

Convection induced by buoyancy force is weak, through it causes overall flow by the nature of body force, and the resultant penetration is similar to the contour line produced by pure heat conduction. In case of surface tension driven convection, the penetration shape is quite different depending on the sign of temperature coefficient. Namely, in case of negative coefficient, the velocity field consists of two flow loops of opposite directions, i.e., one near the weld pool surface and the other in the bulk weld pool, while in case of positive temperature coefficient, fluid flow on the weld pool surface is radially inward, and fluid flow near the center is downward to the weld root which leads to a deep penetration shape.

The convection induced by electromagnetic force re-

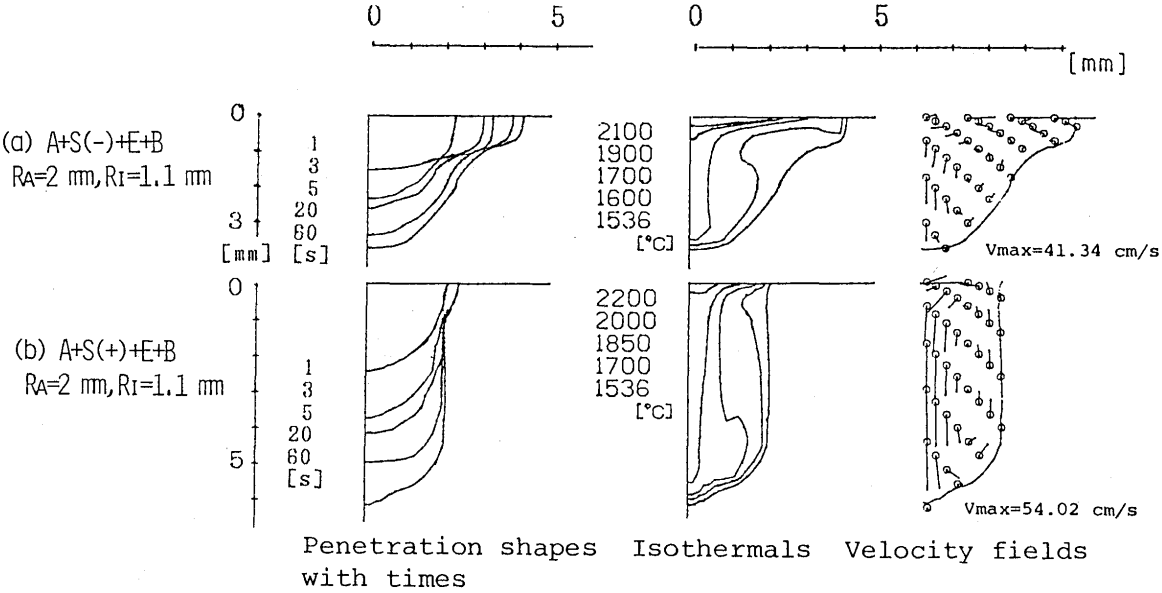

Fig. 6 Penetration shapes with times, temperature and velocity fields due to combined buoyancy force, electromagnetic force and surface tension (including both (a) negative and (b) positive temperature coefficients of surface tension) and aero dynamic drag force for the case : Q = 1570J/s, I = 200A.

sults in a deep and narrow penetration even under the condition of R_I = 2 mm.

In case of the convection driven by aero dynamic drag force, the velocity field consists of two flow loops of opposite direction, i.e., one near the weld pool surface and the other in the bulk weld pool.

Namely, the existence of dual loops in molten pool is a characteristic feature when a radial outward flow is driven by shear stress on the liquid surface.

Figure 6 shows the combined effects of four forces including S(−) and S(+) on the penetration shape, isothermals and velocity fields.

The case of small R_A and R_I, under S(+), resulted in a deep and narrow penetration. On the other hand, in case of S(−), due to three combined effects except for B, the velocity field consists of two flow loops, which leads to a comparatively deep penetration shape.

Figures 7 and 8 show changes of penetration shapes, heat and velocity fields due to individual or combined effects of each motive force respectively for the case of comparatively wide radius of heat and anode source, i.e., R_A = 5 mm, R_I = 5 mm. Convection induced by B and E is very week though it causes overall flow by the nature of body force, and the resultant penetration represents a shape similar to contour produced by pure heat conduction. In case of S(−), there apears complex flow patterns and the penetration shape resembles to that made by pure heat conduction. In case of the convection induced by aero dynamic drag force, the fluid flow on the weld pool surface is radially outward and convection is uniform in the molten pool. Thus, in case of the combined effects of four motive forces under the long arc condition, aero dynamic drag force seems to be more influential than other factors, resulting in a 'shallow' center and 'deep' peripheral penetration.

5. Summary

Four motive forces influencing the weld pool convection were taken into account and their individual and combined contribution to penetration shape were compared.

1) If the arc length is short, the convection of plasma is confined just beneath the cathode tip, while, in case of the long arc length, there found the development of uniform streaming that flows out from inlet to outlet along anode surface; and thus the longer the arc length is, the wider the shear stress of plasma stream acts on liquid surface in the molten pool.
2) When arc length is comparatively long; under the condition of widely distributed heat and current source, the wide shear stress distributions on liquid surface causes a uniformaly strong outward surface flow in the molten pool and produces a 'shallow' center and 'deep' peripheral penetration. A calculated result reproduced well the features of actual TIG penetration.
3) When arc length is comparatively short, that is, in case

C: pure heat conduction, B: byoyancy force, E: electromagnetic force, S(−) & S(+): negative & possitive temperature coefficient of surface tension, A: aero dynamic drag force.

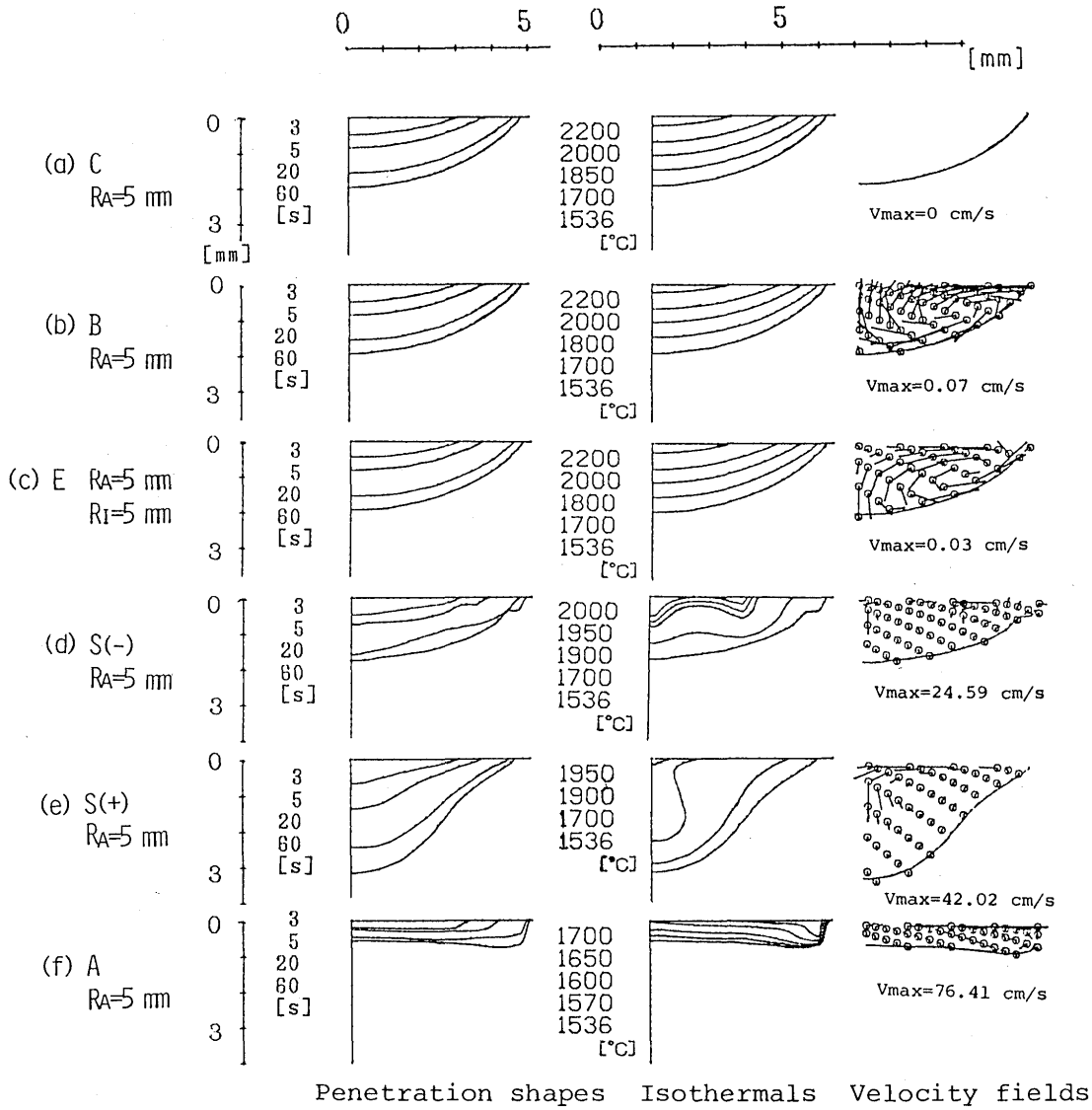

Fig. 7 Individual effect of each motive force for the case: Q = 1570J/s, I = 200A, respectively.

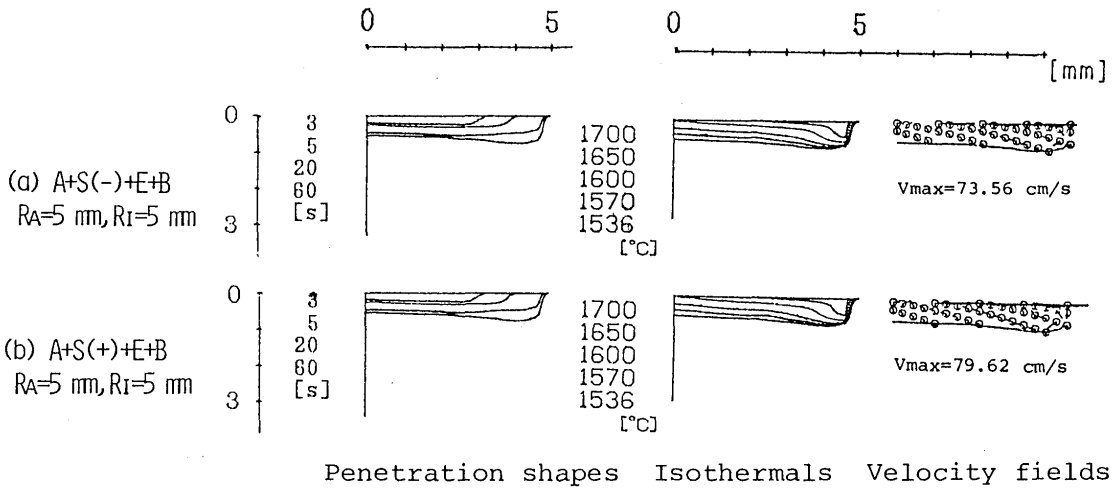

Fig. 8 Combined effect of four motive force for the case: Q = 1570J/s, I = 200A.

of highly concentrated heat and current source, the velocity field consists of two flow loops of opposite directions, i.e., one near the weld pool surface and the other in the bulk weld pool, which lead to relatively deep penetration shape. Also, surface tension of positive temperature coefficient or electromagnetic force takes an important part in flow field as well as penetration shape.

4) The flow speed caused by surface shear stress such as aero dynamic drag force and surface tension are fastest and almost same magnitude. On the other hand the flow induced by body force like electromagnetic force is secondary, and buoyancy force is the weakest among all.

5) Change of fusion boundary were obtained from arc initiation to quasi-stationary state (after about 60 sec), and it was found that the heat flux and flow mode give profound effect on penetration shape of weld pool.

Acknowledgement

The authors express their appreciation to Prof. Ishizaki of Nippon Institute of Technology for his valuable suggestion and discussion.

References

1) Yokoya, S., Asako, Y. and Matsunawa, A., "Surface Tension Driven Flow in Semicylindrical Basin", Trans. J. W. S. Vol. 14, No. 2, 1983.

2) Yokoya, S. and Matsunawa, A., "Surface Tension Driven Flow in Semicylindrical Basin", IIW, Doc-212-568, 1983.

3) Yokoya, S. and Matsunawa, A., "Surface Tension Driven Flow in Hemispherical Basin", Journ. J. W. S., Vol. 2, No. 3 (1984), p. 404 (in Japanese).

4) Oreper, G. M., Eager, T. W. and Szekely, j., "Convection in arc weld pools", W. J., 62, 307s (1983)

5) Oreper, G. M. and Szekely, J. "Heat- and Fluid-flow phenomena in weld pools", J. Fluid Mech (1984), vol. 147 pp53-79.

6) Kou, Sindo. and Sun, D.K., "Fluid flow and weld penetration in stationary arc welds", Metallugical Transactions A 16A. February 1985-203

7) Nisiguchi, K., and Ooji, N.: "Heat transport phenomena in arc welding", JIW WG Arc physics 86-623. (in Japanese)

8) Patanker, S. V., Numerical Heat Transfer, 4, 409, 1981

9) Sozou, C. and Pickering, W. M., "Magnetrohydrodynamic flow in a container due to the discharge of an electric current from a finite size electrode", Proc. Royal Soc. London A, 362, 509 (1978)

10) Mills, K. C., Keene, B. J., Brooks, R. F., and Olusanya, A. 1984. "Surface tension of 304 and 316 type stainless steels and their effect on weld penetration", Report of the National Physical Laboratory, Teddinton, Middlesex, TW11 OLW., UK.

11) Steel handbook "Table 4.9 Heat properties of steel" Maruzen, Inc p. 213. (in Japanease)